Journal of Environmental Protection, 2020, 11, 215-240
https://www.scirp.org/journal/jep
ISSN Online: 2152-2219
ISSN Print: 2152-2197

Mesoscale Impacts on Cold Season $PM_{2.5}$ in the Yukon Flats

Stanley G. Edwin[1,2], Nicole Mölders[2,3]

[1]Council of Athabascan Tribal Governments, Fort Yukon, USA
[2]Department of Atmospheric Sciences, College of Natural Science and Mathematics, University of Alaska Fairbanks, Fairbanks, USA
[3]Geophysical Institute, University of Alaska Fairbanks, Fairbanks, USA
Email: sedwin@alaska.edu, cmoelders@alaska.edu

How to cite this paper: Edwin, S.G. and Mölders, N. (2020) Mesoscale Impacts on Cold Season $PM_{2.5}$ in the Yukon Flats. *Journal of Environmental Protection*, **11**, 215-240.
https://doi.org/10.4236/jep.2020.113013

Received: January 25, 2020
Accepted: March 10, 2020
Published: March 13, 2020

Copyright © 2020 by author(s) and Scientific Research Publishing Inc.
This work is licensed under the Creative Commons Attribution International License (CC BY 4.0).
http://creativecommons.org/licenses/by/4.0/
Open Access

Abstract

Near-surface $PM_{2.5}$ and meteorological observations were performed in three rural communities in the high latitude Yukon Flats valley at various times during the cold season (October to April). These data were synthesized with data from other meteorological sites, NCEP reanalysis and MAIAC retrieved aerosol optical depths data to analyze the role of mesoscale processes and radiation on air quality. Under weak large-scale forcing mountain-valley circulations develop that are driven by the differences in insolation. During the long dark nights, radiative cooling occurs in the near-surface layer of the mountain slopes of the Brooks, Ogilvie and White Mountains Ranges and at the bottom of the valley. Here surface-based inversions (SBI)—known as roof-top inversions—forms, while the cold air drains from the slopes. A frontal wedge forms when the cold air slides over the relatively colder air in the valley. Drainage of cold air from the Brooks Range governed the circulation and cold air pooling in the valley. Concentrations during times with and without SBI differed significantly (at 95% confidence) at two sites indicating that local emissions were the major contributor. At the site, which is closest to the mountains, concentrations marginally changed in the presence of inversions. At all sites, 24-h mean $PM_{2.5}$ remained below the National Ambient Air Quality Standard.

Keywords

Yukon Flats Air Quality, Winter Roof-Top Inversions, High Latitudes, Mesoscale Circulations, Radiative Cooling, Cold Air Pooling, Aerosols, $PM_{2.5}$

1. Introduction

Being mostly located north of the Arctic Circle, the Yukon Flats in Interior

Alaska receive little to no insolation from late November to late January, for which radiative cooling may lead to multi-day surface-based temperature inversions (SBI) wherein pollutants may accumulate over time [1] [2]. Besides such local causes, some large-scale synoptic conditions can cause temperature inversions. An upper level thermal inversion, for instance, can exist at the top of the local atmospheric boundary layer (ABL) [3]. A recent study using radiosonde data showed that in Interior Alaska, SBIs occurred 64% of the time between January 2000 and December 2009 [4]. An SBI occurred with one, two, three, or four simultaneous elevated inversions (EI) 84.86%, 48.49%, 21.23%, and 7.99% of the time, respectively. The mean heights of SBI and the up to four EIs were 377, 1231, 2125, 2720, and 3125 m, respectively. On average, when an SBI was present, the first EI layer occurred at 1249 m under anticyclonic conditions and at 1049 m under warm-air-advection 35.8% and 22% of the time, respectively [4]. Another 23.4% of the inversions occurred under combined synoptic situations, and 18.8% were unclassified. Furthermore, inversion depth, temperature gradient, and frequency showed multi-decadal variations in Interior Alaska [5]. Based on tower observations, [6] found the height of the SBI below 16 m in Fairbanks, also located in the Interior, but in the Tanana Valley south of the Yukon Flats. Note that this height is typically below the first recordings from radiosondes.

Due to the large size of the Yukon Flats, all these different mechanisms for the development of SBI may occur. The Yukon Flats valley is surrounded by mountain ranges with the Brooks Range to the north, and the lower, in height, White Mountain Range to the south, and the Ogilvie Range to the east. Various small indigenous communities reside in the Yukon Flats valley and practice a subsistence lifestyle. These communities are the only anthropogenic emission sources in a wide radius. The majority of the residents in these villages use woodstoves and #1 diesel-burning heaters to heat their homes. Modern offices use diesel furnaces, and electrical power is generated by diesel-burning generators. In the villages, gas-burning vehicles and snow mobiles are the main mean of transportation during winter. All these ways of transportation, heat and energy generation emit particular matter of 2.5 μm or less in diameter ($PM_{2.5}$) along with precursor gases that may lead to formation of $PM_{2.5}$. Obviously, the presence of a SBI reduces or even suppresses the exchange of air with air aloft. Thus, the residents may be exposed to high concentrations of $PM_{2.5}$ ($[PM_{2.5}]$) from their own activities.

Various studies showed relationships between exposure to high $[PM_{2.5}]$ and health conditions [7]. Even in high latitude cities, increases in emergency-room visits, hospitalization, and mortality in elderly people as well as persons with cardiological and/or asthma related pre-conditions were found during events with elevated $[PM_{2.5}]$ [8] [9] [10].

Despite the Yukon Flats are Interior Alaska's largest valley, no radiosonde sites and only three surface meteorological sites exist. No pollution observations exist except for some recent $PM_{2.5}$ measurements performed at four sites and

black carbon measurements at two sites during one wildfire season (mid-May to mid-September) [11] [12]. The reasons for the lack of air-quality measurements in the Yukon Flats are manifold. The valley has sparse population. Most communities are off the Alaska road network and hence difficult and expensive to reach. In winter, the only way to get into or out of the communities is by air travel [13].

A recent study showed that north of 60 N, winter air quality is worse in communities with less than 1000 inhabitants than in cities with population of 10,000 or more [14]. Fairbanks, a community of 31,644 inhabitants [15], is known to exceed the 2006 established US National Ambient Air Quality Standard (NAAQS) [16] of 35 $\mu g \cdot m^{-3}$ for the 24-h average $PM_{2.5}$ concentration several times each cold season (November to February) [17]. Thus, a major concern of the Yukon Flats residents is that during winter, aerosol concentrations could increase to unhealthy level within their communities as well.

A recent climate assessment study reported that the Interior is affected harder and faster by the changes in climate than other regions in the United States [18]. Consequently, due to the lack of historical air-quality baseline data in the Yukon Flats, vulnerability assessment of climate-caused decreases in air-quality and health, as well as developing climate-adaption plans for the future are very difficult.

The goal of this study was to examine the role of mesoscale atmospheric conditions for $PM_{2.5}$ concentrations ($[PM_{2.5}]$) in the Yukon Flats, Alaska. To achieve this goal, concentrations of $PM_{2.5}$ and near-surface meteorological variables were measured in Ts'aahudaaneekk'onh Den (Beaver), Jałgiitsik (Chalkyitsik), and Danzhit Khànlą̨į̨ (Circle) during various months of the 2017 and 2018 cold seasons (October 1 to April 30). The analysis of the measurements included the 1) determination of the frequency and length of SBI occurrence, 2) determination of the $PM_{2.5}$ concentrations during conditions with and without SBI, and 3) identification of the meteorological mechanisms behind the causes of low level SBIs for these communities.

2. Experimental Design

2.1. Air Quality Network and Site Equipment

The Yukon Flats valley has two major river drainages: The Porcupine, and Yukon; draining into the valley from the north-east and out in the south-west; allowing a narrow surface entry and exit between the mountain ranges (**Figure 1**). These three places are the only locations where air from neighboring airsheds can enter or exit the Yukon Flats air shed except when air is mixed down from layers aloft. Therefore, to assess the flow of air in and out of the Yukon Flats, the villages (Circle 65.82569N, 144.0639W, 179 m Chalkyitsik 66.65222N, 143.7258W, 160.5 m) close to these major river inlets and the outlet (Beaver 66.35972N, 147.3975W, 111 m) were chosen as observational sites for meteorology and $PM_{2.5}$. Except Circle, the communities are north of the Arctic Circle (66.56311N).

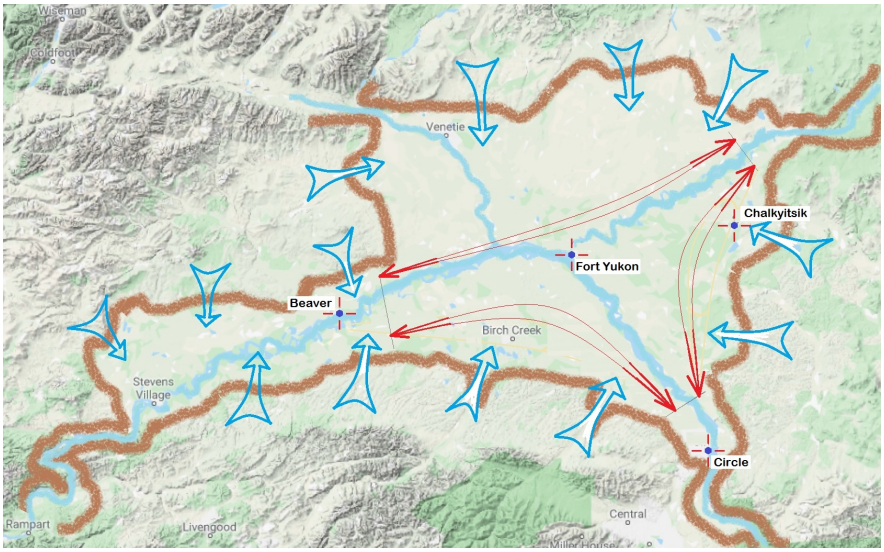

Figure 1. Schematic view of the river drainage system in the Yukon Flats valley (brown lines) and the Brooks Range, Ogilvie Range and White Mountain Range to its the north, east and south. Dots in the crosses are locations of air quality and surface meteorological sites. Red and blue arrows indicate the mountain-valley wind system and slope winds. See section 3 for discussion of wind circulations. Mean distances are about 84 km in N-S and 180 km in W-E direction.

All three sites were equipped with Met One Instruments' BAM-1022, and Decagon's EM50, which are an EPA-suggested equivalent method. To protect the air-intake vents from horizontally blown snow and/or dust, and solar radiation, if any, the BAMs were housed in a box. A tube reaching outside the box took in air at 2 m height. The BAM's BGI VSCC Very Sharp Cut Cyclone (BX-808) particle-size separator was set to permit only particles of 2.5 μm or less to pass.

A Davis Cup Anemometer measured wind speed and direction at 10 m height. Air temperature, pressure, and relative humidity were measured by Decagon EM50 monitors and by a 597 combination sensor at 10 m and 2 m height, respectively. Total incoming radiation was observed at these levels as well. Precipitation was observed at 5 m height. Met One Instruments BAM 1022 PM mass-concentration monitors served to measure $PM_{2.5}$ concentrations. Data accuracy of wind speed, wind direction, relative humidity, air temperature, pressure, and [$PM_{2.5}$] is ±5%, ±7%, ±0.8%, ±0.1˚C, ±0.30 hPa, and ±0.1 μg·m^{-3}, respectively.

These instruments were chosen as they require minimal maintenance. This aspect is of great importance in winter field campaigns in hard to reach locations [12] like the communities in the Yukon Flats. Except Circle all communities are off the Alaska road network.

2.2. Data and Data Processing

The real-time time measurement interval was set to 5 minutes for all devices. Due to the frequent outages that are common in rural communities, many data were missing. Due to the harsh weather conditions, the temperatures in the

housing for the BAM 1022 PM became too low for reliable measurements. After daylight returned, housings were upgraded with heating devices to ensure proper operation.

Data files were synchronized and underwent the quality assurance/quality control (QA/QC) protocol as described in [11]. Data used in this study are April 13, 2017 0000 AKST to April 30, 2017, March 20, 2018 1100 AKST to April 30, 2018 2300 AKST for Circle; March 22, 2018 0000 AKST to April 30, 2018 2300 AKST for Beaver; and April 27, 2017 1300 AKST to April 30, 2300 AKST, October 1, 2017 0000 AKST to October 17, 2017 0900 AKST and February 16, 2018 900 AKST to April 30, 2018 2300 AKST for Chalkyitsik. Sporadically, data were available for the early part of the 2017/2018 cold season. They were examined whether they showed similar behavior as those data that represented the conditions after the Sun raised above the horizon after winter solstice.

Further data processing included calculation of hourly, daily and monthly means and standard deviations for all observed parameters. We used the standard deviation to assess the temporal variations [19].

To distinguish between cases with and without SBI within the limits of our available data and monitoring heights, the vertical temperature gradient between the temperature measurements at 10-m and 2-m height was determined for every hour using the hourly data.

We used the NCEP reanalysis data to assess the impact of the synoptic scale forcing on the meteorological situations in the valley. Since clouds affect, among other things, solar downward radiation reaching the surface and near-surface temperature, we also examined the ceiling heights observed at the National Weather Service sites in Arctic Village (Vashrąįį K', 68.121828N, 145.527686W, 638 m) and Fort Yukon (Gwichyaa Zhee 66.56667N, 145.2581W, 138 m).

Multi-Angle Implementation of Atmospheric Correction (MAIAC) retrieved aerosol optical depth (AOD) data from Moderate Spectral Distribution Spectrometer (MODIS) [20] on board of the Aqua and Terra satellites were downloaded from the LAADS archive for 150W to 143W, 65N to 67.8N for the total 2017/18 cold season (October 1 to April 30).

2.3. Data Analysis

Daily 24-h averages of $PM_{2.5}$ were examined for exceedance of the NAAQS of 35 $\mu g \cdot m^{-3}$ recommended by the US Environmental Protection Agency (EPA) [16] and the 3-day mean of 25 $\mu g \cdot m^{-3}$ recommended by the World Health Organization (WHO) [21].

The signs of the temperature gradient data were examined to distinguish between hours with (positive sign) and without (negative sign) SBI. Then the $PM_{2.5}$ concentrations during times with and without SBIs were examined to assess the background concentrations and degree of pollution. Furthermore, inversion length and frequency were calculated.

Due to the lack of winter radio-soundings, we compared the 2-m air temper-

atures observed at Arctic Village and Fort Yukon to examine whether there were EI over the Yukon Flats. The latter community is in the center of the valley, while the former is on the foothills of the Brooks Range north of Ft. Yukon (Figure 1).

During winter in Interior Alaska, so-called low roof-top inversions blanket small communities. Typically, smoke from residential and commercial heating reaches above these inversions (Figure 2). To assess whether in the Yukon Flats valley, these inversions retard accumulation of pollutants and/or shield the communities from locally sourced and/or advected concentrations of $PM_{2.5}$ ($[PM_{2.5}]$) of hours with and without temperature inversions between 10-m and 2-m height were compared. By using changes in monitored physical properties between two heights as a comparative, the meteorological mechanism for the inversions by location in the valley and their impacts on local winter air quality were examined.

The MAIAC data were used to assess the mean AOD and temporal and spatial distribution of aerosols over the Yukon Flats over a cold season.

3. Results and Discussion

The Yukon Flats encompass about 28,490 km^2 with extended wetlands and about 40,000 small lakes and streams. The region is protected under the Yukon Flats National Wildlife Refuge. The Yukon Flats have strong continental sub-arctic climate (Köppen-Geiger classification Dfc) [22]. Winters are very severe with temperature often dropping below −57˚C, while summers often see 35˚C. The record low temperature was −61.1˚C in Ft. Yukon in December 1917; the highest temperature on record was 37.8˚C on June 27, 1915.

Figure 2. Photo showing exemplarily a SBI at Chalkyitsik. At the top of the SBI, haze can be seen. The exhaust from most chimneys is buyoant and hot enough to reach levels above the SBI. Photo taken March 1, 2018.

3.1. Emissions in the Yukon Flats

In the villages, fixed emission sources burning grade-1 diesel are the power plant, laundry-mat, city office buildings, corporation buildings, businesses, school and support buildings, the Tribal Council and Tribal Consortium buildings; and if existent, the clinic. Emissions from residential heating stem from both furnaces burning grade-1 diesel and woodstoves. In addition, emissions from open wood-fires for cooking dog food exist; typically, they occur in the evening in winter. Emissions from heating decrease with increasing air temperature and vice versa [11].

In Ft. Yukon, Beaver and Chalkyitsik, passenger cars, trucks and heavy equipment exist despite there is no access to the Alaska road network. In all communities, traffic emissions stem from gas and diesel engines. Given the low temperatures, cold starts lead to high emissions [23]; idling to warm up the engine is common in the cold season. Off-road traffic emissions stem from four-wheelers and snow mobiles. Typically, emissions from traffic decrease with increasing air temperature and vice versa [11].

All villages have an airport with daily flights except Ft. Yukon where multiple flights occur daily. Aircrafts use leaded fuel due to the high octane requirement. **Figure 3** exemplarily shows the annual emission totals from airport emissions for various communities in the Yukon Flats. For details on the emission sources see [11].

Other sources of aerosols are the village road systems, dust from river gravel bars [14] (in fall and late spring) and secondary particles due to gas-to-particle conversion and sublimation/evaporation of haze, cloud and precipitation particles.

3.2. Meteorological Conditions

3.2.1. Insolation

Figure 4(a) shows the solar climate at the top of the atmosphere (TOA) over the four villages in the Yukon Flats, Arctic Village on the slope of the Brooks Range

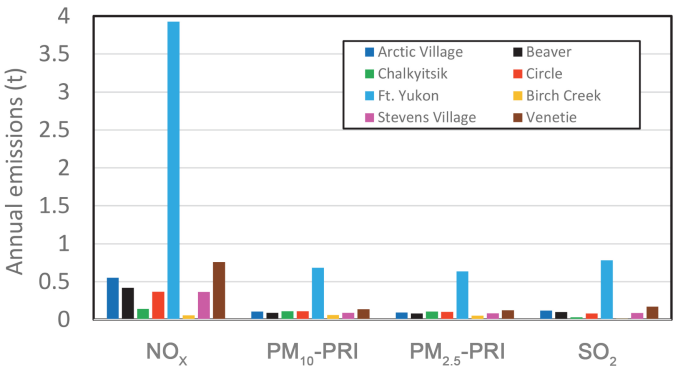

Figure 3. Airport emissions of particulate matter pre-cursor gases sulfur dioxide (SO_2) and nitrogen oxides (NO_x) and primary $PM_{2.5}$ and particulate matter less than 10 μm in diameter (PM_{10}) in various communities of the Yukon Flats for 2017. Units are metric tons.

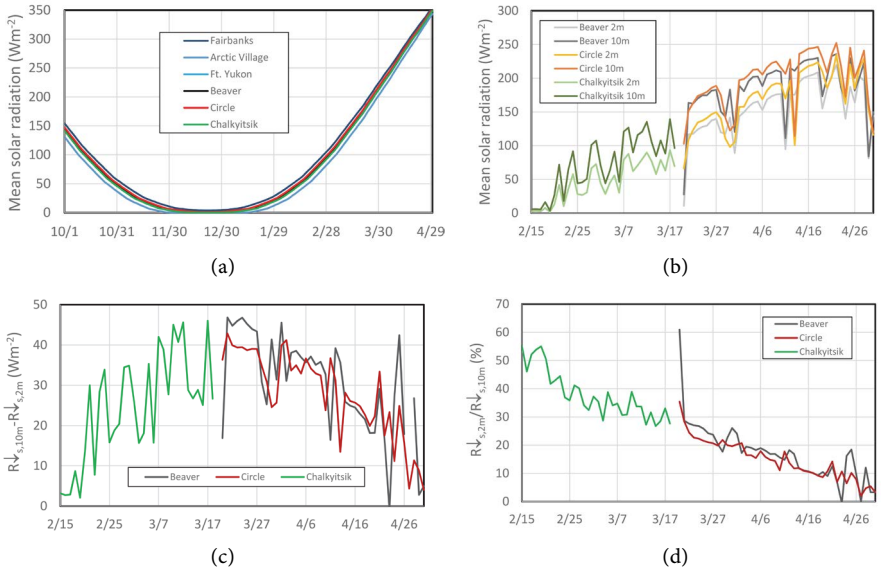

Figure 4. (a) Daily mean downward solar radiation at the top of the atmosphere (TOA) for the four villages and for comparison Arctic Village located on the slope of the Brooks Range and Fairbanks located south of the White Mountain Range in the Tanana Valley; (b) Zoom-in on daily mean solar radiation as observed at selected sites at 2-m and 10-m after the Sun rises again above the horizon; Ratios of (c) observed daily mean downward solar radiation at 10-m height over the daily mean downward solar radiation at the TOA; and (d) observed daily mean downward solar radiation at 2-m height over 10-m height. Values for Chalkyitsik represent a different time period than those for Beaver and Circle.

and for comparison Fairbanks (64.8378N, 147.7164W) calculated for the cold season (October 1 to April 30). Even Circle barely has any insolation around winter solstice.

Figure 4(b) shows exemplarily the shortwave downward radiation at 2-m and 10-m height as observed in Beaver, Chalkyitsik and Circle towards the end of the cold season. At all sites, incoming solar radiation was lower when a low pressure system went over the region. Slight temporal offsets occurred due to the different locations. As expected, on average, near-surface solar radiation was higher in the farther south than farther northern locations (**Figure 1**, **Figure 4(a)**).

The comparison of the near-surface shortwave downward radiation and that at the TOA revealed the following. At all sites, the total amount of solar radiation absorbed between the TOA and 10-m above the ground level (AGL) increased with increasing insolation (compare **Figure 4(a)** and **Figure 4(b)**). Even during times without frontal passages, notable absorption of solar radiation occurred between the TOA and the surface sites. On average over all available data, the near-surface shortwave downward radiation was 75.2, 38.6 and 66.2 $W \cdot m^{-2}$ lower than at the TOA for Beaver, Chalkyitsik and Circle, respectively. This means at these sites, on average, near-surface shortwave downward radiation was about 27%, 43% and 24% of the respective values at the TOA (**Figure 4(c)**).

Incoming solar radiation at 10-m and 2-m heights correlated about 90%, 95% and 99% at Beaver, Circle and Chalkyitsik, respectively. Typically, at all sites,

incoming solar radiation at 10-m was notably higher than at 2-m height above ground level (Figure 4(d)). Even during frontal passages differences occurred. On average over all available observations, differences were 30.3, 28.1 and 24.7 $W \cdot m^{-2}$ at Beaver, Circle and Chalkyitsik, respectively. The percentage of solar radiation absorbed between 10-m and 2-m decreased with increasing solar radiation (Figure 4(d)).

Together these observations suggest that notable amounts of absorbing gases, particles and potentially water droplets and/or ice existed between 10-m and 2-m height. These findings can be explained by local emissions of pollutants and water vapor that accumulated under SBIs (Figure 3, Figure 5, Figure 6).

3.2.2. Temperature Inversions

The gradient between the 2-m air temperatures at Arctic Village and Ft. Yukon served as a proxy for the "vertical" temperature gradient over the Yukon Flats. Comparing the hourly meteorological conditions at Ft. Yukon and Arctic Village revealed the following. During the October to April 2017/18 cold season, mean 10-m wind speeds and 2-m temperatures were 1.67 $m \cdot s^{-1}$, −14.8˚C and 1.62 $m \cdot s^{-1}$, −16.4˚C at the sites in 138 m and 638 m above sea-level (ASL), respectively. Mean sea-level pressure was about 1019.43 hPa. In March and April, 10-m wind speeds increased. Such increase in March wind speed was also found for Fairbanks [24] [25] [26].

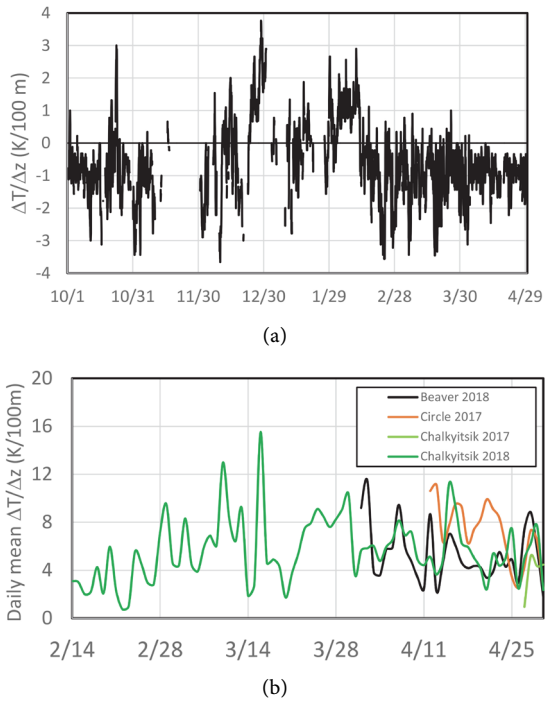

Figure 5. (a) Hourly mean vertical temperature gradient between the National Weather Service sites at Arctic Village (638 m) and Ft. Yukon airport (138 m) from October 1, 2017 to April 30, 2018; (b) Daily mean temperature gradient as observed between 10-m and 2-m during SBI at Beaver, Circle and Chalkyitsik during various campaigns. The latter was expressed in K per 100 m for easy comparison of inversion strengths.

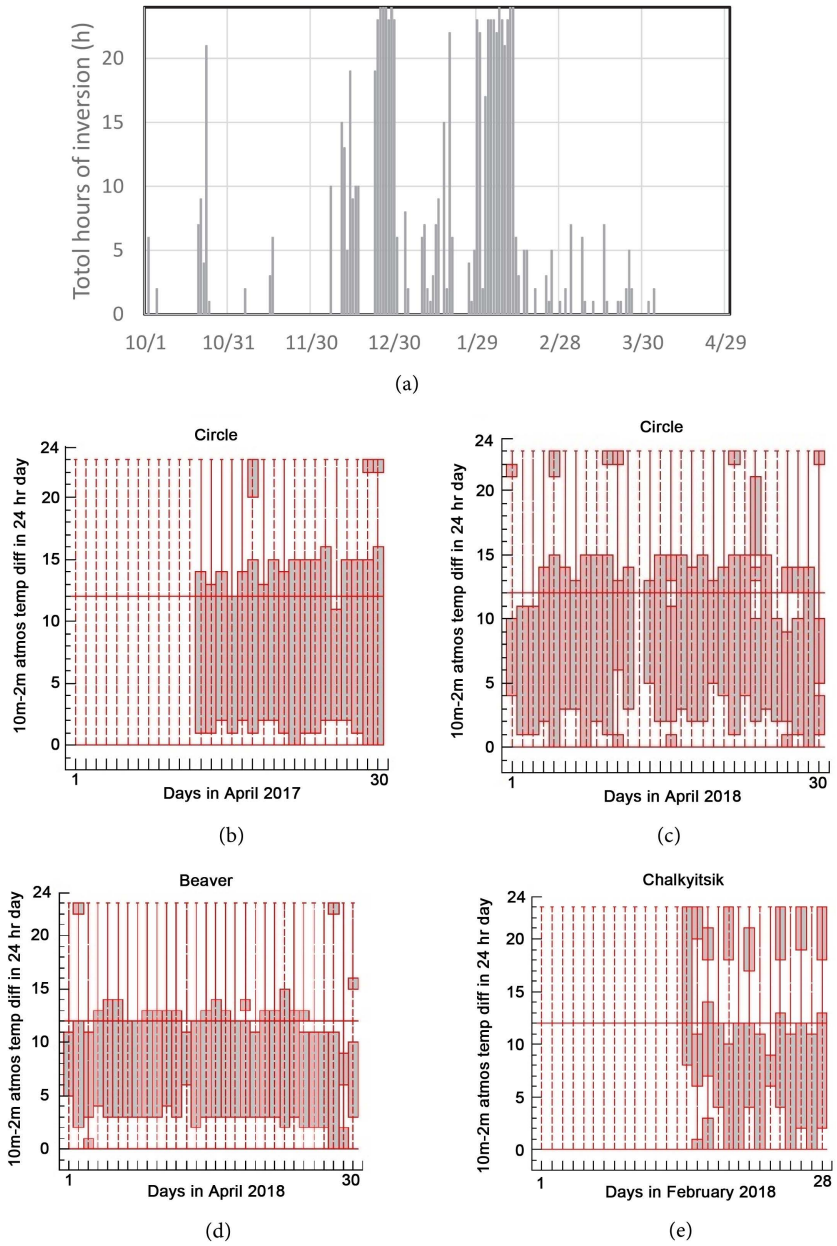

Figure 6. Temporal distribution of daily mean temperature gradient during SBI between 10 m and 2 m as obtained for (a) February 1 to April 30 at various sites, and Hovmüller plots of inversion times (gray shading) as observed at Circle in April (b) 2017; (c) 2018; (d) Beaver in April 2018, and (e) Chalkyitsik in February 2018. Note that SBIs occurred daily. Days with missing data are left blank in (b) to (e).

During inversions over the Yukon Flats, the mean temperature gradient was 1.07·(100 m)$^{-1}$, and −1.11·(100 m)$^{-1}$ otherwise. On average over all data, the temperature gradient was −0.63 K·(100 m)$^{-1}$, *i.e.* close to the mean environmental lapse rate. During the times without insolation, the inversions between 638 m and 138 m were the strongest reaching up to 3.76 K·(100 m)$^{-1}$ (Figure 5). On cold season average, the temperature gradient was 1.07 K·(100 m^{-1}) and −1.11 K·(100 m^{-1}) during times with and without inversions, respectively. The strong-

est decrease of temperature with height was −3.66 K·(100 m^{-1}), which hints at conditions with nearly height-constant density.

The frequency and duration of inversions over the Yukon Flats increased as insolation decreased towards winter solstice and as time without insolation continued thereafter (cf. **Figure 4**, **Figure 5**). After the Sun raised above the horizon again, inversion duration and frequency decreased (cf. **Figure 4**, **Figure 6**). Typically, the strongest and longest inversions coincided with no or only weak insolation at the TOA (**Figures 4-6**). On daily average, the total duration of inversions between 638 m and 138 m was 3.8 h.

The 10-m to 2-m temperature-gradient data revealed that low SBIs developed daily over the villages in the Yukon Flats through the night and lasted into late morning (e.g. **Figure 6**). The duration of SBIs increased as insolation decreased. The opposite was true when the Sun raised again above the horizon and insolation increased (cf. **Figure 4**, **Figure 6**). Note that this pattern also was found for the time after and before summer solstice [11].

Daily mean durations of inversions were 9.43 h (Beaver), 10.60 h (Chalkyitsik) and 13.33 h (Circle). During SBIs, the daily mean temperature gradients were 5.35·(100 m)$^{-1}$, 5.53·(100 m)$^{-1}$ and 7.19 K·(100 m)$^{-1}$ for Beaver, Chalkyitsik, and Circle, respectively. On average, the strength and length of these SBIs exceeded the strength and length of inversions found over the Yukon Flats.

The temperature gradients between Arctic Village and Ft. Yukon indicated temperature inversions, isothermal and no inversion conditions for about 21%, 2% and 77% of the data, respectively (**Figure 5(a)**). Obviously, in the Yukon Flats, the frequency for SBI was higher than the 68.5% and 74.9% reported for Fairbanks during the November to February cold seasons of 1957-2008 [5] and 1999-2009 [17], respectively. This finding can be explained by the farther north location and hence lower insolation and greater radiation loss in the Yukon Flats than at Fairbanks during the cold season.

Over the Yukon Flats, about 2%, 8% and 11% of the observations showed an increase of temperature with height under negative, no and positive vertical wind shear conditions. Isothermal conditions occurred for 2% of the observations. In about 21%, 19% and 36% of the data, temperature decreased with height under negative, no and positive wind shear conditions. Vertical wind shear was negative, zero and positive 39%, 28% and 33% of the time, respectively. The negative shear indicates the impact of topography like channeling of the wind field.

3.2.3. Ceiling

Analysis of the cloud ceiling data from Arctic Village and Ft. Yukon indicated cloud-free conditions for about 57% of the time. Arctic Village is located 500 m higher than Ft. Yukon. Normalizing to height ASL revealed that the percentage of cloud ceilings above 838 ASL showed quite different behavior, while those between 638 and 838 m agreed well (**Figure 7**). When looking at ceilings with respect to height above ground level (AGL), the percentage of ceilings above 700 m AGL showed similar decrease at both villages. This finding can be related to

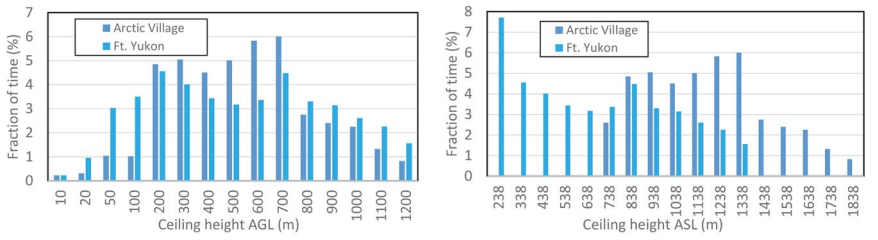

(a) (b)

Figure 7. Percentage of time with various ceiling heights at the National Weather Service site at Ft. Yukon airport (138 m) and Arctic Village (638 m) from October 1, 2017 to April 30, 2018 (a) as reported above ground level and (b) expressed with respect to sea level height.

large-scale systems and lifting/descending of the air mass over/from the mountain range.

At Ft. Yukon, ceilings below 100 m occurred nearly three times as often than at Arctic Village, while ceilings between 100 and 200 m had about the same percentage of occurrence (**Figure 7**). Such low level haze layers may occur when relatively warmer, moist air is lifted over relatively colder air. At Arctic Village, ceilings above 20 m and below 700 m AGL seemed to be governed by local topographic forcing.

3.2.4. Air Motions and Cold Air Pooling

Under weak synoptic scale forcing, local classical mesoscale mountain-valley wind circulation systems and downslope winds developed (**Figure 1**). According to the observations, cold air drained from the slopes of the Brooks Range, the White Mountain Range and the Ogilvie Range and built a cold air pool in the valley. Despite the low insolation (cf. **Figure 4**), reduced heat loss during twilight and increased heat loss at night were sufficient to produce differential heating between the upper and lower part of the valley floor. Thus, along the line of the Porcupine- and Yukon rivers a mountain-valley flow established (**Figure 1**) that turned its direction after onset of twilight and after twilight ended (**Figure 8**).

Various large lakes exist close to Beaver and Chalkyitsik. All rivers and lakes were frozen and snow covered. The Yukon is more than 3.5 km wide at Circle, 3 km wide at Ft. Yukon, 6 km at Beaver; the Porcupine is about 60 m at Chalkyitsik and about 800 m before it splits into its upper and lower mouth at Ft. Yukon. Both rivers meander strongly and have many sloughs and bogs. Thus, the high albedo of the snow-covered frozen waters and riverbanks as compared to the low albedo of the boreal forest contributed to radiative cooling. Consequently, the cold air mass got channeled along the Porcupine to its mouth and from there downstream along the Yukon (**Figure 1**).

Under weak large-scale forcing, mountain-valley wind systems formed parallel to the Ogilvie Range, south slope of the Brooks Range and the north slope of the White Mountain Range (**Figure 1**). **Figure 8(a)** exemplarily shows the change in wind direction in the diurnal course during times with weak large-scale

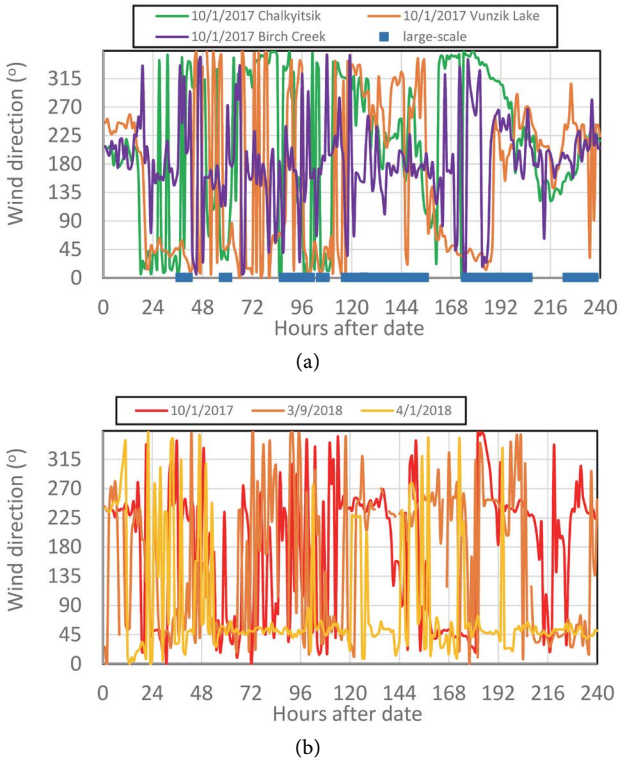

Figure 8. Examples of 10-d timeseries of hourly wind direction at (a) various sites in the Yukon Flats starting October 1, 2017, and (b) Beaver starting October 1-10, 2017, March 9, 2018 and April 1, 2018. Plots for other sites and times look similar. Blue bars in (a) indicate times of distinct large-scale forcing.

forcing. **Figure 8(b)** exemplarily illustrates that such mountain-valley circulations occurred at various times during the cold season.

Close to the outlet of the Yukon from the Yukon Flat, as well as between Beaver and Ft. Yukon, and between Ft. Yukon and Circle, the slope of the White Mountain Range is exposed broadly to the southwest, east-east north-east and east-south east, respectively. Thus, before and after the total lack of insolation (**Figure 4**) differences in surface heating may cause this mountain-valley wind system under weak synoptic forcing conditions. For the mountain-valley wind system along the Ogilvie Range, the earlier onset no insolation and later return of insolation at the northern than southern locations may cause the small temperature, density and pressure differences that drive the system.

Arctic Village is the only observational site located on a slope. On average, the 2-m temperatures at Arctic Village were −5.5 K lower and 5.3 K higher than at Ft. Yukon for 77% and 21% of the time, respectively. During inversions, a cold air pool formed on the valley floor. The limited vertical extend and strong SBI (**Figure 5**) restricted the vertical motion.

During night, air close to slopes cools faster than air at the same height over valley [27]. The cold air drained down the slopes. This air slightly differed in density and/or temperature from that in the valley. Thus, these two air masses of different characteristics formed a cold surface front wedge. Herein the cold-

er/drier air was pushed under the comparatively warmer/moister air, resulting in a SBI. Recall that at Beaver, Chalkyitsik and Circle inversions existed for a couple of hours each day (e.g. **Figure 5**).

Obviously, the duration of the SBI and the constant wind just above) with a direction parallel along the mountain range/valley boundary (**Figure 1**) depended on distance from the mountains. The distances to the mountains in N, E, S, W directions are about 18, 76, 16, and 17 km at Beaver, 25, 1.6, 0, 128 km at Chalkyitsik, 29, 5, 15, and 11 km at Circle, and 48, 64, 51 and 74 km at Ft. Yukon, respectively. A greater distance from the mountains means a larger pool and reservoir of cold surface air as compared to close to the White Mountain and Ogilvie ranges.

There were also cases of cold air downslope-flow inversions that occurred without the topography channeling the winds along the valley surface as well as classic SBI due to radiative cooling.

The mountain-valley circulations were perpendicular to downslope flow (**Figure 1**). Thus, concurrent existence of slope winds and mountain-valley winds may initiate vorticity [27]. Such vorticity generation due to slope winds from the Alaska Range and mountain-valley winds was found to be one of the pre-requisites for ABL funnel clouds in the Tanana Flats Valley during summer [28].

In the Tanana Flats valley near Fairbanks, winter SBI were 16 m on average [6]. The three times higher frequency of ceilings below 20 m at Ft. Yukon than Arctic Village (**Figure 7**) suggests that the cold air pool on the bottom of the Yukon Flats valley most likely had only several tenth of meter in vertical extension as well.

The reanalysis revealed five distinct situations of downslope cold air flow and cold air pooling. In the following, we discuss exemplarily the five days from April 1 to April 5, 2018, which are representative of all the meteorological situations when downslope drainage and cold air pooling created SBIs (**Figure 9**). The 2-m temperature reanalysis data showed a strong influence of the Chandalar River inlet into the Yukon Flats Valley. It acts as a channel for the downslope cold air flow into the Yukon Flats off the southern slope of the Brooks Range. The cold air moved towards Ft. Yukon. Therefore, Ft. Yukon typically had colder conditions than the surrounding villages. Note that e Chandalar River has no connection to an outside air shed.

In the case of an SBI, the maximum difference between the measured 10-m and 2-m temperature indicates the proximity to the meteorological cause of the SBI during the cold season. **Figure 10** shows the situation where cold air drainage from the Brooks Range occurred through the Chandalar River canyon toward Ft. Yukon. In this case, the SBI occurred first in Chalkyitsik. Here the greatest difference between the 10-m and 2-m temperatures was the largest of the three villages. The maximum difference observed in Chalkyitsik during the cold season was 10 K.

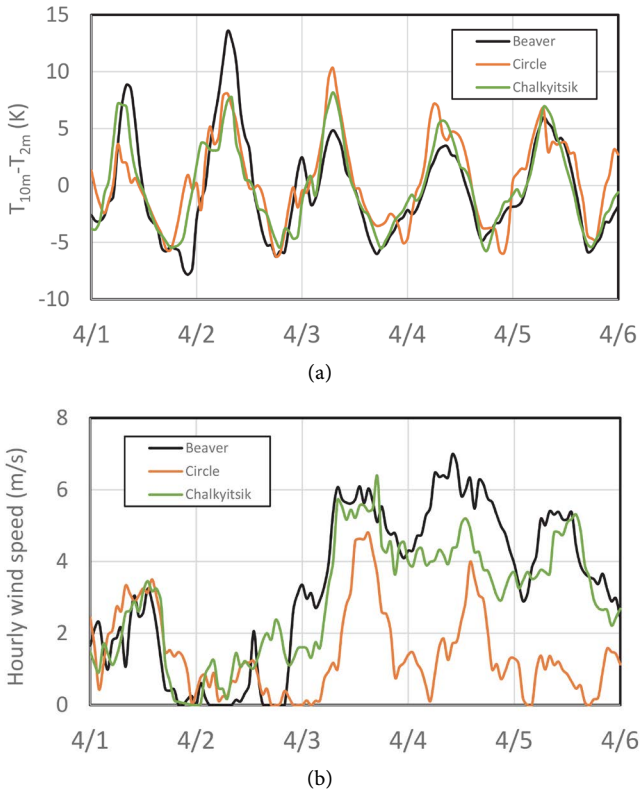

Figure 9. April 1, 0000 Alaska Standard Time (AKST) to April 6 0000 AKST, 2018 hourly means of (a) difference between 10-m and 2-m temperatures and (b) 10-m wind speeds at Beaver, Chalkyitsik and Circle.

The SBI occurred on average an hour later in Circle with a slightly lower temperature difference between the 10-m and 2-m temperatures due to mixing with the ambient air that was replaced by the cold air drainage. Once reaching Beaver another hour later, the temperature difference was 5 K. This means that the SBI strength decreased with increasing distance from the origin of the cold air drainage. In this type of event, the 10-m wind speed was initially very weak (<2 $m \cdot s^{-1}$) when the cold air arrived at a village. In Chalkyitsik and Circle, the wind speed was about 3.5 $m \cdot s^{-1}$ when the SBI ended around noon (**Figure 9**). On the contrary, at Beaver, the SBI ended about an hour later at similar 10-m wind speeds as observed for Chalkyitsik and Circle.

Figure 11 shows the case when cold air moved down the Chandalar River watershed and led to cold air pooling. The pattern with respect to temperature difference (**Figure 9**) and the difference in timing when the SBI was seen at the village, was similar to the event of April 1.

However, the initial wind speed was less than for April 1. This type of event led to an earlier onset of the SBI that was created by the drainage flow with a longer duration than for April 1. As the flow stopped, a cold pool remained and prolonged the duration of the SBI (**Figure 9**). The SBI finally dissipated during the day due to solar heating and a change in the overall wind direction in the Yukon Flats.

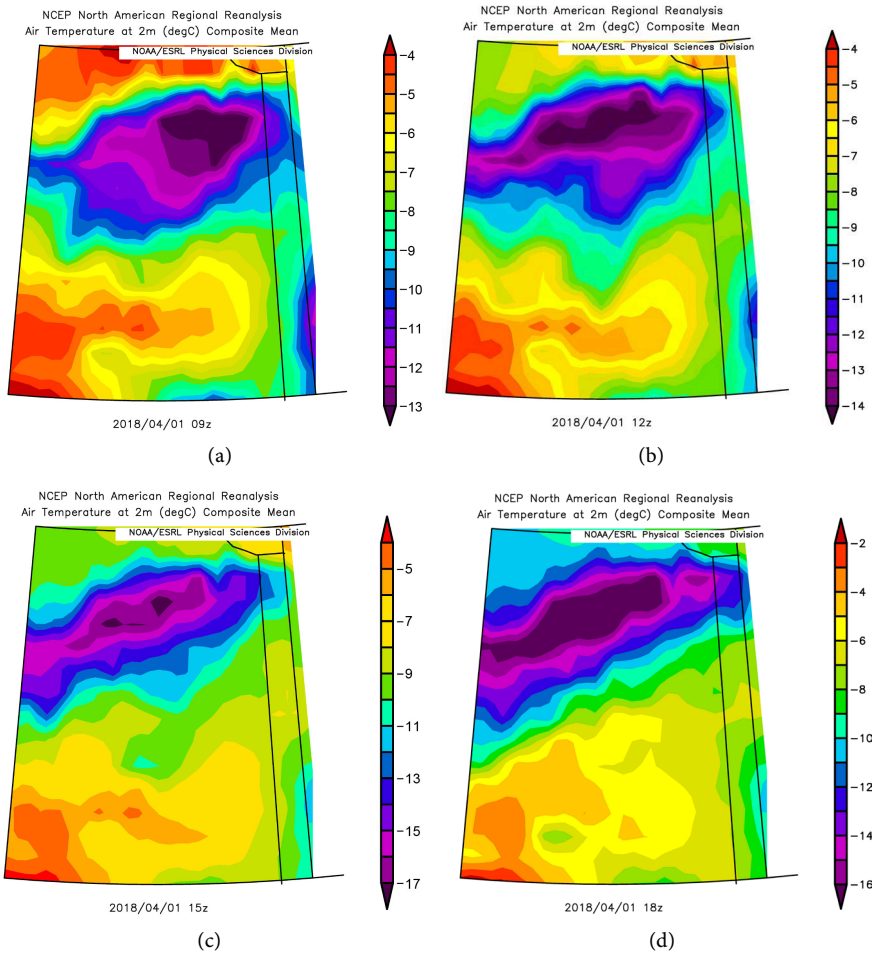

Figure 10. Reanalysis data of 2-m height temperature on April 1, 2018 over the Yukon Flats, Brooks Range, Ogilvie Range and White Mountain Range at (a) 0100 AKST; (b) 0400 AKST; (c) 0700 AKST; (d) 1000 AKST.

April 3, 2018 (**Figure 12**) is an example where cold air drainage occurred from all mountain ranges (Brooks Range, Ogilvie Range, White Mountain Range). Thus, the relatively warmer air in the Yukon Flats was lifted as a whole. The large scale near-surface winds were weak from the North. The SBI dissipated when near-surface winds increased during the day (**Figure 9**).

April 4, 2018 (**Figure 13**) represents the case where cold pooling occurred right at the slope of the White Mountain Range. At the beginning, cold air drained from the Brooks Range into the Yukon Flats. The onset was seen at the same time in Chalkyitsik and Beaver. Once the drainage flow stopped, the SBI remained due the cold pool. However, the cold pool occurred more to the southwest of Ft. Yukon than on April 2 when the wind came from the northwest. On April 4, however, winds were sporadic and from north easterly directions except for Circle where they were westerly right from the Yukon Flats.

April 5 (**Figure 14**) is similar to the cases with drainage from the Brooks Range and formation of a cold pool. However, during this event temperatures decreased more than 10 K (**Figure 9**). The large-scale near-surface wind came

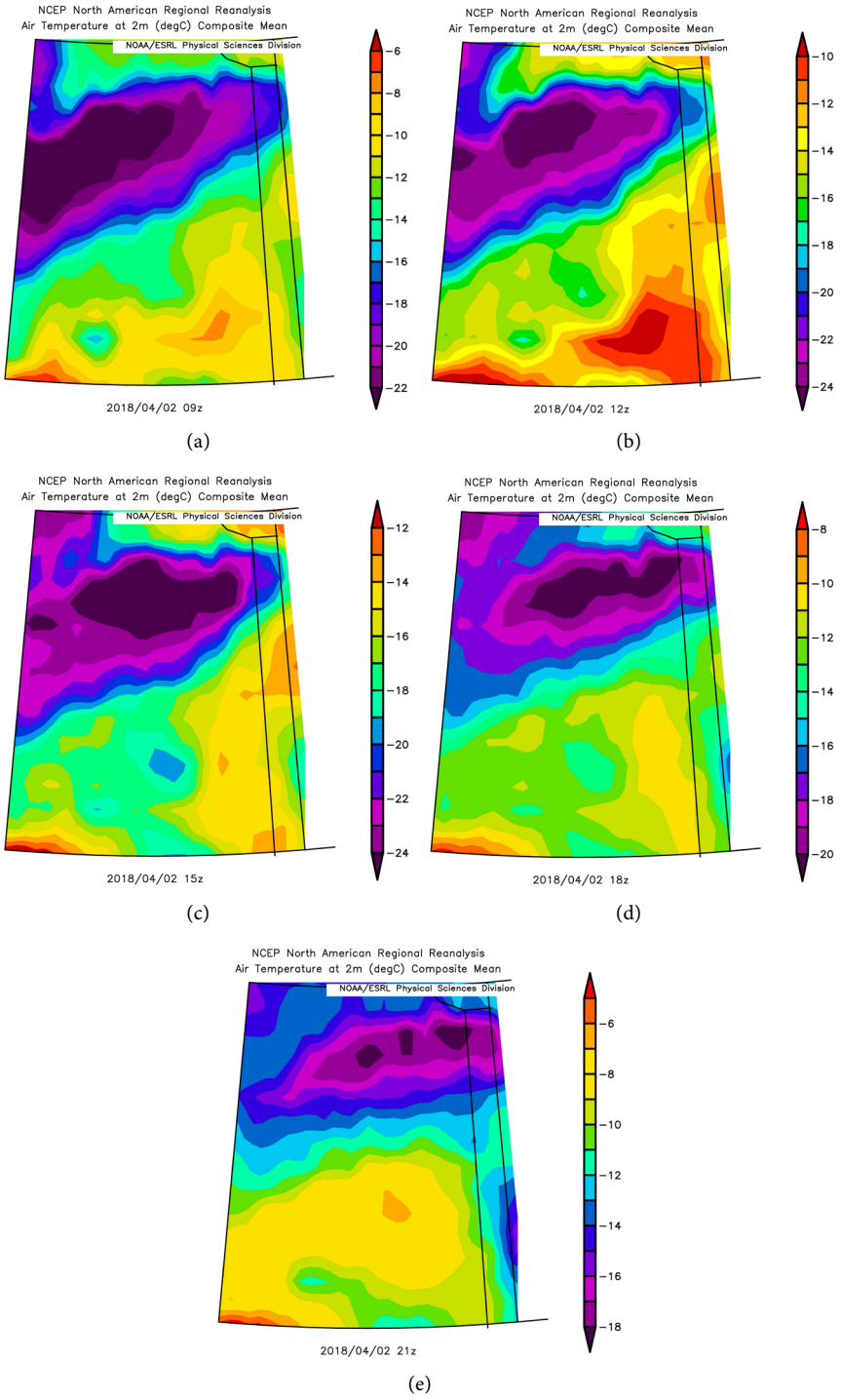

Figure 11. Reanalysis data of 2-m height temperature on April 2, 2018 over the Yukon Flats, Brooks Range, Oglivie Ranage and White Mountain Range at (a) 0100 AKST; (b) 0400 AKST; (c) 7 AKST; (d) 1000 AKST; and (e) 1300 AKST.

from east-northeasterly directions. However, the cold pool had its center with the lowest temperatures between Ft. Yukon, Chalkyitsik and Circle in the early morning (**Figure 14**). In the next three hours, the cold pool moved towards the Steven Village area, while warming notably due to solar heating. Due to the

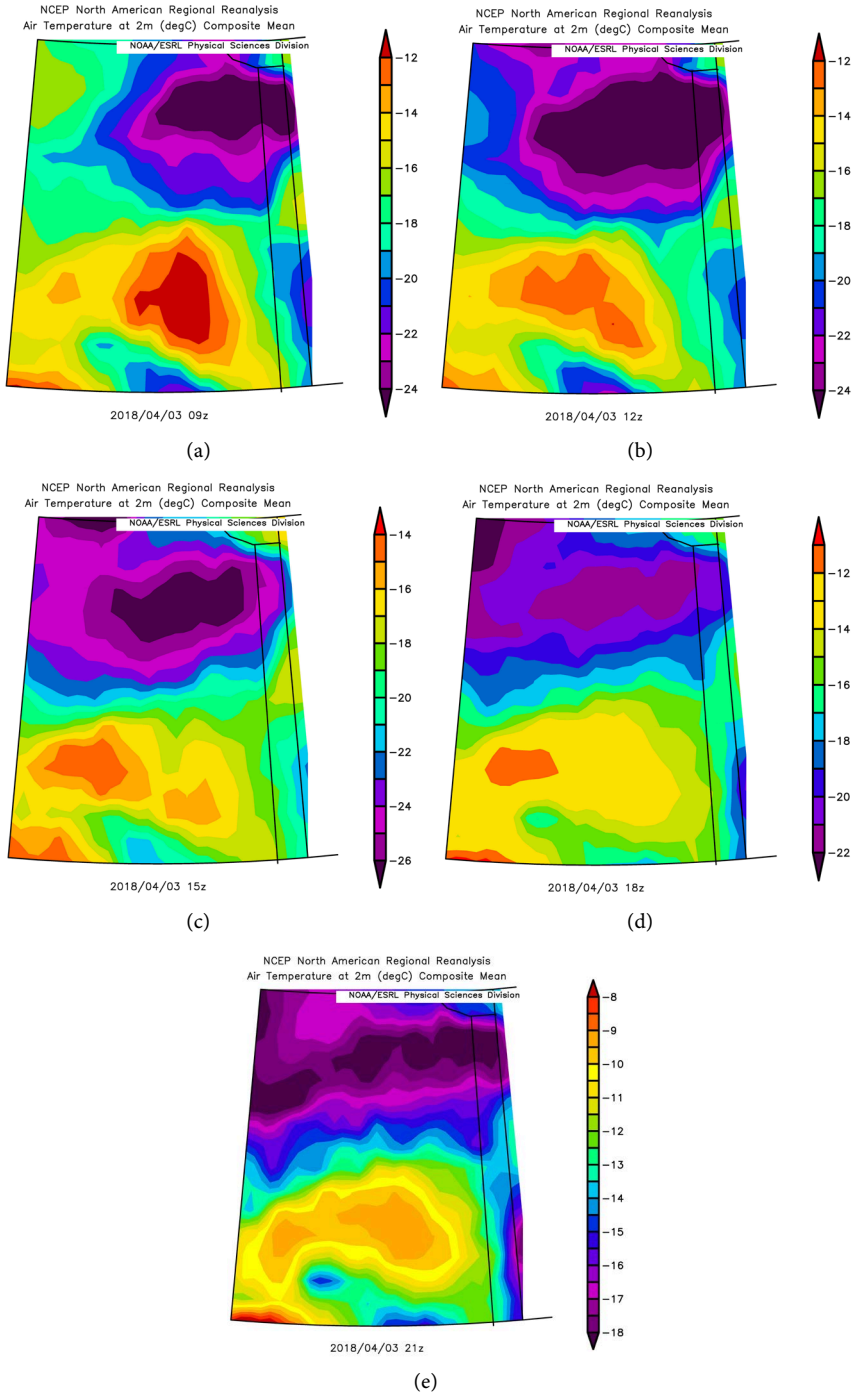

Figure 12. Reanalysis data of 2-m height temperature on April 3, 2018 over the Yukon Flats, Brooks Range, Oglivie Ranage and White Mountain Range at (a) 0100 AKST; (b) 0400 AKST; (c) 0700 AKST; (d) 1000 AKST; and (e) 1300 AKST.

extremely low temperature of the cold pool, the SBI lasted longer into the day than for the other cases with a lasting cold pool after the drainage stopped. Relatively warmer air moved along the Ogilvie Range northward around the cold pool and terminated the SBIs with Circle being the first, Chalkyitsik next followed by Beaver.

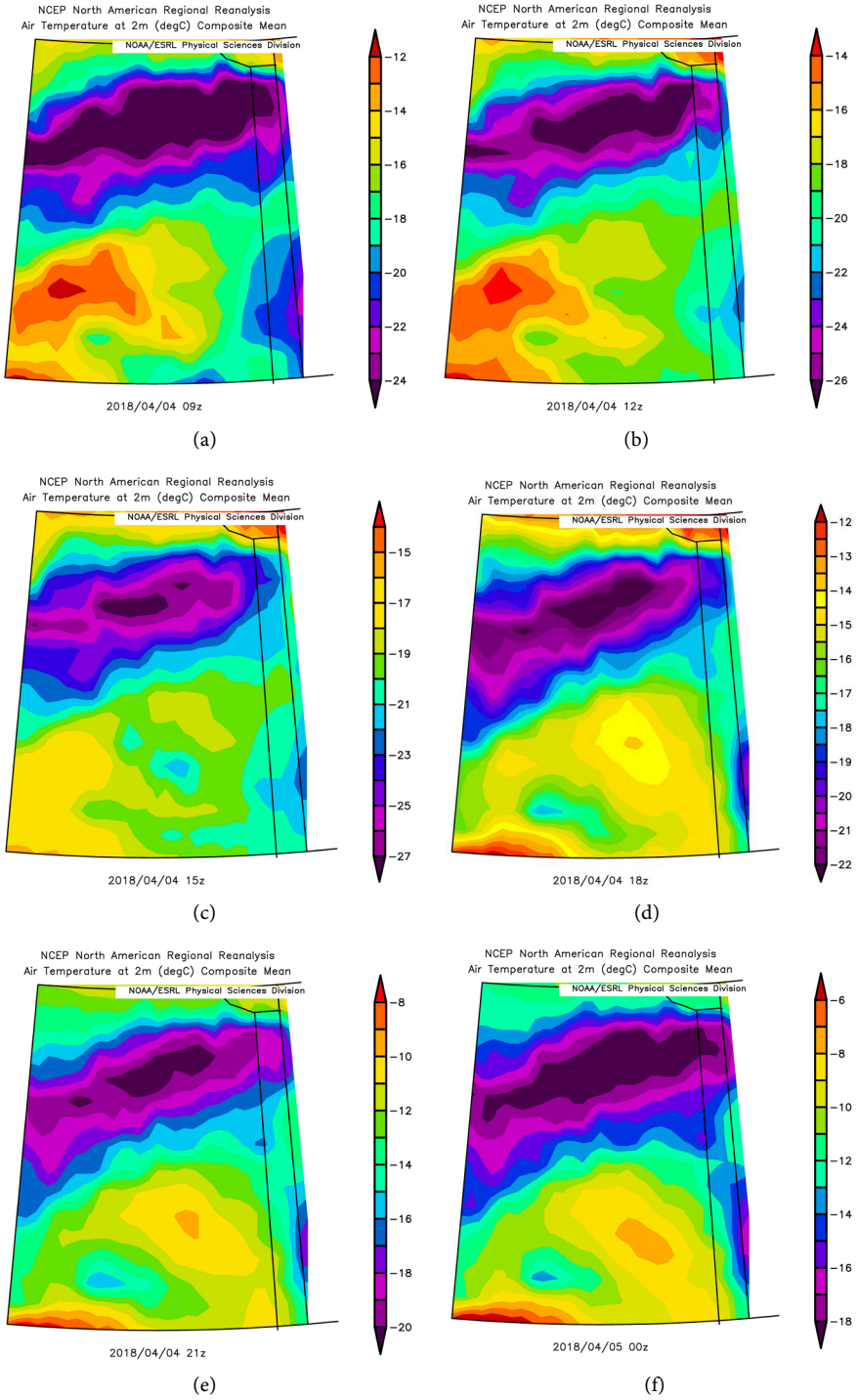

Figure 13. Reanalysis data of 2-m height temperature on April 4, 2018 over the Yukon Flats, Brooks Range, Oglivie Ranage and White Mountain Range at (a) 0100 AKST; (b) 0400 AKST; (c) 0700 AKST; (d) 1000 AKST; (e) 1300 AKST and (f) 1600 AKST.

The reanalysis revealed that during the cold season under weak large scale forcing, the Brooks Range governs the duration of the SBIs and the mesoscale dynamics in the Yukon Flats. The direction of the large-scale flow governs which of the circulation patterns establishes and hence the duration of the SBIs.

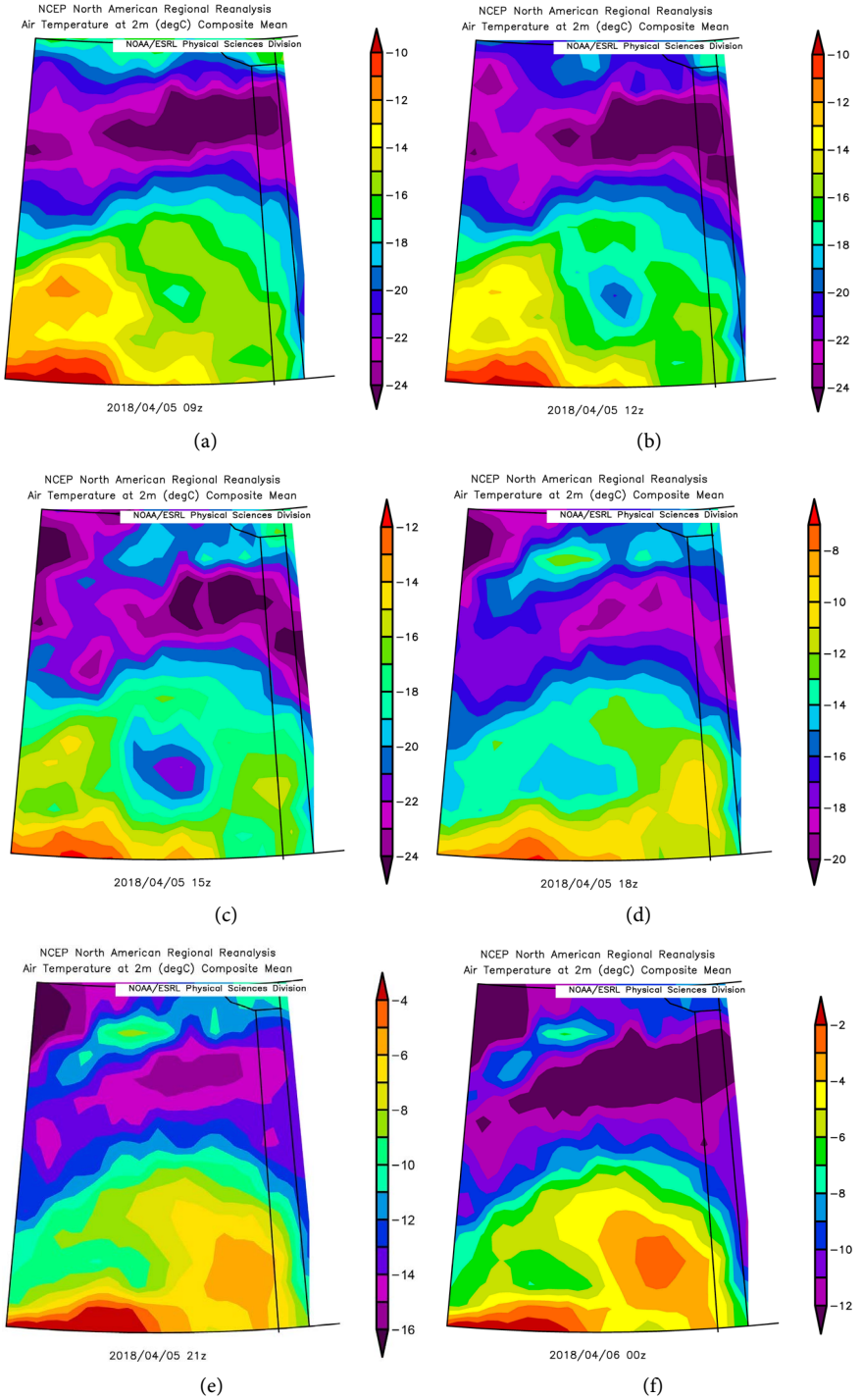

Figure 14. Reanalysis data of 2-m height temperature on April 5 over the Yukon Flats, Brooks Range, Oglivie Ranage and White Mountain Range at (a) 0100 AKST; (b) 0400 AKST; (c) 0700 AKST; (d) 1000 AKST; (e) 1300 AKST and (f) 1600 AKST.

3.3. Concentrations of $PM_{2.5}$ and Aerosol Optical Depth

Figure 15 shows the aerosol optical depth determined over the Yukon Flats for the length of the 2017/18 cold season. Typically mean AOD was between 0.2 and 0.5 except for a few times with distinct, high values. Frequency of high AOD

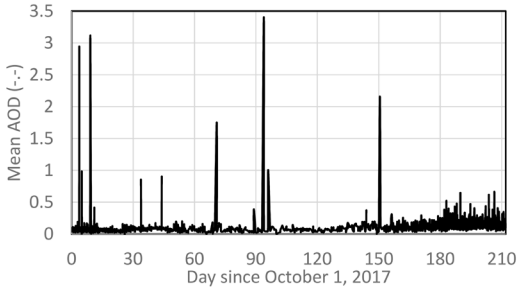

Figure 15. Temporal evolution of mean AOD over the area as determined from all Aqua and Terra paths with valid data; for the 2017/18 cold season.

increased with progressing time. HYSPLIT [29] backward trajectories and reanalysis data suggested transport of aerosol from mid-latitudes. Such impacts of air mass advection on AOD were also found over Gotland (Baltic Sea) [30].

Daily means, medians and 98 percentile of AOD were smallest during polar night and slightly increased with progressing time towards spring (**Figure 15**). In 12% of the cases, the daily median exceeded the daily mean. Maximum AOD notably decreased as time progressed in the cold season. Daily standard deviations of AOD showed no notable tendency. Area-averaged monthly means and standard deviations were 0.08 ± 0.07, 0.09 ± 0.07, 0.08 ± 0.07, 0.13 ± 0.06, 0.13 ± 0.07, 0.12 ± 0.07 and 0.17 ± 0.06 for October 2017 to April 2018, respectively; monthly means of daily maximum AOD were 1.14, 1.07, 1.07, 1.14, 1.30, 1.06, and 0.83. The high October mean of daily maximum AOD was due to some wildfires still burning in Canada and the Yukon Flats, while the high February mean of daily maximum AOD was due to advection. The cold season mean AOD over the area was 0.12 ± 0.17.

On average, near-surface observed $PM_{2.5}$ concentrations were higher in 2018 than 2017 (**Table 1**). In Chalkyitsik, which is the closest to the mountains (cf. **Figure 1**), the variations in $PM_{2.5}$ were higher in 2018 than 2017 as well. In April 2017 and 2018, mean overall $PM_{2.5}$ concentrations were highest at Chalkyitsik and about twice as high than in Circle (**Figure 16**). At Circle, concentrations decreased as temperatures increased and decreased with increasing insolation during times without SBI. On the contrary, at Chalkyitsik, concentrations decreased as temperatures increased and decreased with increasing insolation in general.

In the presence of SBI, at Circle and Chalkyitsik, $PM_{2.5}$ concentrations were on average 1.4 (1.3) $\mu g \cdot m^{-3}$ and 2.4 (0.2) $\mu g \cdot m^{-3}$ higher in 2017 (2018) than under conditions without SBI, respectively. Investigation of daily means of concentrations during hours with SBI and without SBI at Circle revealed a correlation of about 52% and 23% in 2017 and 2018, respectively. A two-tailed, paired Student t-test indicated significant differences with 95% confidence. At Chalkyitsik, correlations of concentrations during times of SBI and no SBI were about 91% and differences were statistically insignificant. This means that air quality was dominated by local sources at Chalkyitsik and the mountain-valley circulation barely affected the concentrations. At Circle, however, during times without SBIs concentrations were significantly diluted.

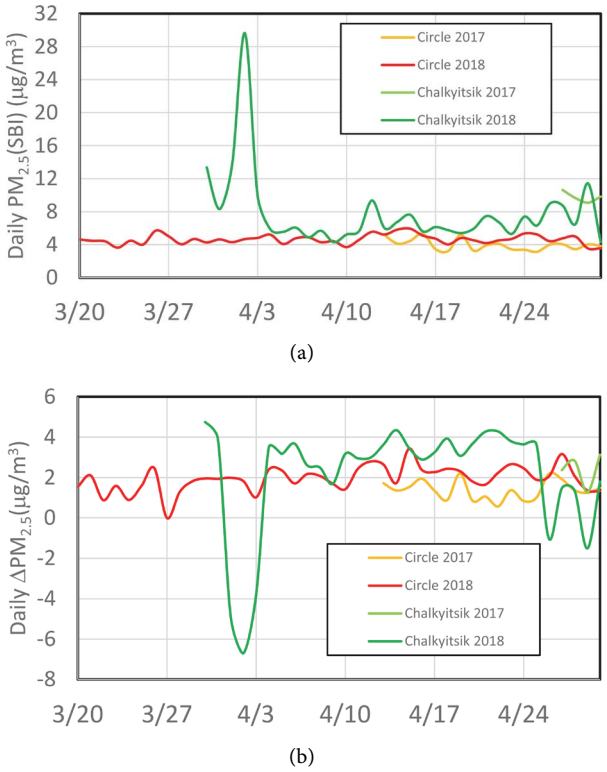

Figure 16. Examples of temporal evolution of daily (a) mean $PM_{2.5}$ concentrations during SBIs and (b) differences between $PM_{2.5}$ concentrations during times with and without SBIs. Plots for other days and Beaver look similar.

Table 1. Cold season mean $PM_{2.5}$ concentrations based on all available data at the sites. Too few data existed for Beaver in 2017 for a reasonable statistic (therefore not listed).

Location	Characteristics of cold season hourly $PM_{2.5}$ concentrations		
	Overall ($\mu g \cdot m^{-3}$)	No SBI ($\mu g \cdot m^{-3}$)	During SBI ($\mu g \cdot m^{-3}$)
Beaver 2018	11.1 ± 10.7	11.5 ± 11.4	7.9 ± 10.0
Chalkyitsik 2017	8.6 ± 1.3	7.4 ± 0.7	9.8 ± 0.6
Chalkyitsik 2018	9.6 ± 17.1	9.5 ± 22.0	9.7 ± 10.3
Circle 2017	3.2 ± 0.9	2.6 ± 0.5	4.0 ± 0.7
Circle 2018	3.7 ± 1.2	2.7 ± 0.6	4.6 ± 0.6

Monthly means of total aerosol concentration during inversions varied marginally among the months of the cold season. Also monthly mean $PM_{2.5}$ concentrations varied marginal between times when no SBIs and when SBIs were present (Figure 16).

4. Conclusions

Concentrations of $PM_{2.5}$ and near-surface meteorological variables measured in Arctic rural communities in the Yukon Flats in April 2017 and the 2017/18 cold season (October to April) were augmented with surface meteorological data ob-

tained from NCEP and the WRCC, NCEP reanalysis data, and MAIAC aerosol optical depth data as well as simulated solar downward radiation at the TOA. Due to the harsh winter conditions in the Arctic and frequent, often daily outages only sporadic data existed in the early to mid-winter cold season. Based on these experiences, a heating blanket and battery system was designed and first implemented at Circle and later at Beaver.

The reanalysis revealed that during the cold season under weak large-scale forcing, the Brooks Range governed the duration of surface-based inversions and the mesoscale dynamics in the Yukon Flats. Cold air drainage from the Brooks Range caused cold pooling in the valley. The direction of the large-scale flow governed which of the circulation patterns established and hence the duration of the SBIs. The strength of SBIs was determined by the distance from where the cold air drainage occurred.

The reanalysis and meteorological surface observations revealed that under weak large-scale forcing mountain-valley circulations developed along the three mountain ranges that surround the Yukon Flats valley. Radiative cooling led to formation of daily surface-based inversions. The duration of SBIs increased towards winter solstice and decreased after the Sun raised again above the horizon. [$PM_{2.5}$] was significantly (at 95% confidence) higher during hours with SBIs than during hours without SBIs of the same day at Beaver and Circle. Based on this finding, one may conclude that local emissions were the major contributor to the observed [$PM_{2.5}$] except for Chalkyitsik. Here, differences in concentrations were marginal between hours with and without SBIs.

In the Yukon Flats, the tops of SBIs are often visible due to haze or ice fog. Ceiling heights observed at Ft. Yukon (138 m ASL) in the Yukon Flats and Arctic Village (638 m) in the Brooks Range were normalized to sea-level height. This analysis showed that in the valley, ceilings below 20 m occurred more frequently than in the mountains. On the contrary, high ceilings due to large-scale processes showed similar distributions for both sites. Based on these findings one may conclude that in the Yukon Flats, SBIs extended only several decameters in the vertical.

Analysis of the reanalysis data together with the near-surface meteorological data of wind speed, wind direction, shortwave downward radiation near the surface and 2-m and 10-m air temperatures suggested that under weak large-scale forcing, radiative cooling over the mountain slopes yielded to cold air drainage from the slopes.

Under weak large-scale forcing, the wind system in the valley was perpendicular to the downslope descending cold air. This means that air was transported directly across the valley floor and vorticity was generated. This prolonged transport of cold air accounted for the cold season SBIs that were accompanied with increases in $PM_{2.5}$ concentrations as compared to times without inversions at Beaver and Circle. At Chalkyitsik, the polluted air mostly moved back and forth along the mountains. Note that this community is much closer to the mountains than Beaver and Circle.

The analysis revealed that 24-h mean [$PM_{2.5}$] remained below the NAAQS of 35 $\mu g \cdot m^{-3}$. Also the WHO recommended thresholds were not exceeded. The analysis of MAIAC aerosol optical depth featured the presence of aerosols from long-range transport with distinct peaks often an order of magnitude higher than the background values. Under weak large-scale forcing mean AOD was slightly higher in October due to some of the 2017 wildfires still burning/smoldering in parts of the Yukon Flats and Yukon Territory, Canada. Values also increased towards the end of the cold season due to Arctic haze. Daily maximum AOD values reached up to 5 locally. No direct association with the emissions from the rural communities could be made. Based on the measurements, one may conclude that the strong peaks in AOD were due to aerosols at higher atmospheric levels because the concentrations found in the villages well agreed with the local emission and meteorological patterns, but showed no correlation to that of AOD.

Based on this study, the communities in the Yukon Flats still breathe healthy air during the cold seasons. Obviously, advection of polluted air from aloft or through the two inlets and the outlet of the Yukon Flat valley seemed not to occur during the time for which data are available. However, if the communities and hence emissions increase over time, measures to reduce accumulation of pollutants under the SBI might become necessary given the daily occurring inversions. During this first study, unfortunately only sporadic data were taken in deep winter (December, January). Since these are climatologically the coldest months, a study with winterized equipment is recommended.

Acknowledgements

We thank the anonymous reviewers for fruitful discussion and helpful comments, the Tribes of the Yukon Flat villages for permission to carry out the observations in their villages, and the Tribal Resilience Program, NASA grant #80NSSC19K0981 and the State of Alaska for financial support of this study. MODIS aerosol optical depth data were downloaded from the NASA Earth Observatory. The surface meteorological data of the National Weather Service stations were downloaded from the historic global dataset at NCEP.

Conflicts of Interest

The authors declare no conflicts of interest regarding the publication of this paper.

References

[1] Mölders, N. and Kramm, G. (2010) A Case Study on Wintertime Inversions in Interior Alaska with WRF. *Atmospheric Research*, **95**, 314-332. https://doi.org/10.1016/j.atmosres.2009.06.002

[2] Mölders, N., Fochesatto, G.J., Edwin, S.G. and Kramm, G. (2019) Geothermal, Oceanic, Wildfire, Meteorological and Anthropogenic Impacts on $PM_{2.5}$ Concentrations in the Fairbanks Metropolitan Area. *Open Journal of Air Pollution*, **8**, 19-68.

https://doi.org/10.4236/ojap.2019.82002

[3] Fochesatto, G.J. (2015) Methodology for Determining Multilayered Temperature Inversions. *Atmospheric Measurement Techniques*, **8**, 2051-2060. https://doi.org/10.5194/amt-8-2051-2015

[4] Mayfield, J.A. and Fochesatto, J. (2013) The Layered Structure of the Winter Atmospheric Boundary Layer in the Interior of Alaska. *Journal of Applied Meteorology and Climatology*, **52**, 953-973. https://doi.org/10.1175/JAMC-D-12-01.1

[5] Bourne, S.M., Bhatt, U.S., Zhang, J. and Thoman, R. (2010) Surface-Based Temperature Inversions in Alaska from a Climate Perspective. *Atmospheric Research*, **95**, 353-366. https://doi.org/10.1016/j.atmosres.2009.09.013

[6] Wendler, G. and Nicpon, P. (1975) Low-Level Temperature Inversion in Fairbanks, Central Alaska. *Monthly Weather Review*, **103**, 34-44. https://doi.org/10.1175/1520-0493(1975)103<0034:LLTIIF>2.0.CO;2

[7] Sinkemani, R., Sinkemani, A., Li, X. and Chen, R. (2018) Risk of Cardiovascular Disease Associated with the Exposure of Particulate Matter ($PM_{2.5}$): Review. *Journal of Environmental Protection*, **9**, 12. https://doi.org/10.4236/jep.2018.96038

[8] Halonen, J.I., Lanki, T., Yli-Tuomi, T., Kulmala, M., Tiittanen, P. and Pekkanen, J. (2008) Urban Air Pollution and Asthma and Copd Hospital Emergency Room Visits. *Thorax*, **63**, 635-641. https://doi.org/10.1136/thx.2007.091371

[9] Segersson, D., Eneroth, K., Gidhagen, L., Johansson, C., Omstedt, G., Nylén, A.E., *et al.* (2017) Health Impact of PM_{10}, $PM_{2.5}$ and Black Carbon Exposure Due to Different Source Sectors in Stockholm, Gothenburg and Umea, Sweden. *International Journal of Environmental Research and Public Health*, **14**, 742. https://doi.org/10.3390/ijerph14070742

[10] Asikainen, A., Pärjälä, E., Jantunen, M., Tuomisto, J.T. and Sabel, C.E. (2017) Effects of Local Greenhouse Gas Abatement Strategies on Air Pollutant Emissions and on Health in Kuopio, Finland. *Climate*, **5**, 43. https://doi.org/10.3390/cli5020043

[11] Edwin, S.G. and Mölders, N. (2018) Particulate Matter Exposure of Rural Interior Communities as Observed by the First Tribal Air Quality Network in the Yukon Flat. *Journal of Environmental Pollution*, **7**, 223-245. https://doi.org/10.4236/jep.2018.913088

[12] Mölders, N. and Edwin, S.G. (2018) Review of Black Carbon in the Arctic: Origin, Measurement Methods and Observations. *Open Journal of Air Pollution*, **7**, 181-213. https://doi.org/10.4236/ojap.2018.72010

[13] Edwin, S.G. (2016) Climatology and Forcing Mechanism of Funnel Clouds in Alaska. M.S. thesis. Department of Atmospheric Sciences, University of Alaska Fairbanks, Fairbanks, AK.

[14] Mölders, N. and Kramm, G. (2018) Climatology of Air Quality in Arctic Cities-Inventory and Assessment. *Open Journal of Air Pollution*, **7**, 48-93. https://doi.org/10.4236/ojap.2018.71004

[15] Bureau of U.S. Census (2018) National Population Projections.

[16] EPA (2011) National Ambient Air Quality Standards (NAAQS). http://www.epa.gov/air/criteria.html

[17] Tran, H.N.Q. and Mölders, N. (2011) Investigations on Meteorological Conditions for Elevated PM2.5 in Fairbanks, Alaska. *Atmospheric Research*, **99**, 39-49. https://doi.org/10.1016/j.atmosres.2010.08.028

[18] Chapin, F.S.I. (2014) National Climate Assessment-Alaska. U.S. Government, United States of America, 841.

[19] Kim, J., Waliser, D.E., Mattmann, C.A., Mearns, L.O., Goodale, C.E., Hart, A.F., *et al.* (2013) Evaluation of the Surface Climatology over the Conterminous United States in the North American Regional Climate Change Assessment Program Hindcast Experiment Using a Regional Climate Model Evaluation System. *Journal of Climate*, **26**, 5698-5715. https://doi.org/10.1175/JCLI-D-12-00452.1

[20] Lyapustin, A., Wang, Y., Korkin, S. and Huang, D. (2018) MODIS Collection 6 MAIAC Algorithm. *Atmospheric Measurement Techniques*, **11**, 5741-5765. https://doi.org/10.5194/amt-11-5741-2018

[21] WHO (2006) World Health Organization Air Quality Guidelines for Particulate Matter, Ozone, Nitrogen Dioxide and Sulfur Dioxide. In: *Summary of Risk Assessment*, World Health Organization, Geneva, 22.

[22] Mölders, N. (2019) Outdoor Universal Thermal Comfort Index Climatology for Alaska. *Atmospheric and Climate Sciences*, **9**, 26. https://doi.org/10.4236/acs.2019.94036

[23] Weilenmann, M., Favez, J.-Y. and Alvarez, R. (2009) Cold-Start Emissions of Modern Passenger Cars at Different Low Ambient Temperatures and Their Evolution over Vehicle Legislation Categories. *Atmospheric Environment*, **43**, 2419-2429. https://doi.org/10.1016/j.atmosenv.2009.02.005

[24] Shulski, M. and Wendler, G. (2007) The Climate of Alaska. University of Alaska Press, Fairbanks, AK, 216.

[25] Mölders, N. (2013) Investigations on the Impact of Single Direct and Indirect and Multiple Emission-Control Measures on Cold-Season Near-Surface $PM_{2.5}$ Concentrations in Fairbanks, Alaska. *Atmospheric Pollution Research*, **4**, 87-100. https://doi.org/10.5094/APR.2013.009

[26] Malingowski, J., Atkinson, D., Fochesatto, J., Cherry, J. and Stevens, E. (2014) An Observational Study of Radiation Temperature Inversions in Fairbanks, Alaska. *Polar Science*, **8**, 24-39. https://doi.org/10.1016/j.polar.2014.01.002

[27] Mölders, N. and Kramm, G. (2014) Lectures in Meteorology. Springer, Heidelberg, 591. https://doi.org/10.1016/j.polar.2014.01.002

[28] Edwin, S.G., Mölders, N., Friedrich, K., Schmidt, S. and Thoman, R. (2017) Conditions Supporting Funnel Cloud Development in Alaska. *Atmospheric and Climate Sciences*, **7**, 223-245. https://doi.org/10.4236/acs.2017.72016

[29] Draxler, R., Stunder, B., Rolph, G., Stein, A. and Taylor, A. (2009) HYSPLIT4 User's Guide. 231.

[30] Zdun, A., Rozwadowska, A. and Kratzer, S. (2016) The Impact of Air Mass Advection on Aerosol Optical Properties over Gotland (Baltic Sea). *Atmospheric Research*, **182**, 142-155. https://doi.org/10.1016/j.atmosres.2016.07.022